

PCR-99: A Practical Method for Point Cloud Registration with 99 Percent Outliers

Seong Hun Lee¹, Javier Civera² and Patrick Vandewalle³

Abstract—We propose a robust method for point cloud registration that can handle both unknown scales and extreme outlier ratios. Our method, dubbed PCR-99, uses a deterministic 3-point sampling approach with two novel mechanisms that significantly boost the speed: (1) an improved ordering of the samples based on pairwise scale consistency, prioritizing the point correspondences that are more likely to be inliers, and (2) an efficient outlier rejection scheme based on triplet scale consistency, prescreening bad samples and reducing the number of hypotheses to be tested. Our evaluation shows that, up to 98% outlier ratio, the proposed method achieves comparable performance to the state of the art. At 99% outlier ratio, however, it outperforms the state of the art for both known-scale and unknown-scale problems. Especially for the latter, we observe a clear superiority in terms of robustness and speed.

I. INTRODUCTION

We consider the problem of correspondence-based point cloud registration with or without the knowledge of the relative scale, *i.e.*, aligning two corresponding sets of noisy and outlier-contaminated 3D points to obtain the most accurate relative rotation, translation (and scale) between them. This problem is relevant in many applications, such as 3D scene reconstruction [3], [4], object recognition and localization [5], [6], and simultaneous localization and mapping [7].

Unlike the commonly used Iterative Closest Point (ICP) [8], correspondence-based methods have the advantage that they do not rely on the initial guess for the unknown transformation between the two point sets. Instead, they first match 3D keypoints using feature descriptors (*e.g.*, FPFH [9]), and then infer the transformation from the putative correspondences. In practice, however, these correspondences may occasionally contain a large proportion of outliers (*e.g.* more than 95%) [10]. It is therefore important that the estimation method can handle such extreme outlier ratios.

In this work, we propose a novel point cloud registration method that is robust to an extremely large amount of outliers (up to 99%). Our main contribution is two-fold:

- 1) We develop a deterministic approach for choosing 3-point samples in such a way that the inlier correspondences are more likely to be chosen earlier than the outliers. The key idea is to rank each point based on

*This work was supported by the Spanish Government (projects PID2021-127685NB-I00 and TED2021-131150BI00) and the Aragón Government (project DGA-T45 23R).

^{1,2} Seong Hun Lee and Javier Civera are with I3A, University of Zaragoza, 50018 Zaragoza, Spain. seonghunlee@unizar.es, jcivera@unizar.es

³ Patrick Vandewalle is with EAVISE, Department of Electrical Engineering, KU Leuven, 2860 Sint-Katelijne-Waver, Belgium. patrick.vandewalle@kuleuven.be

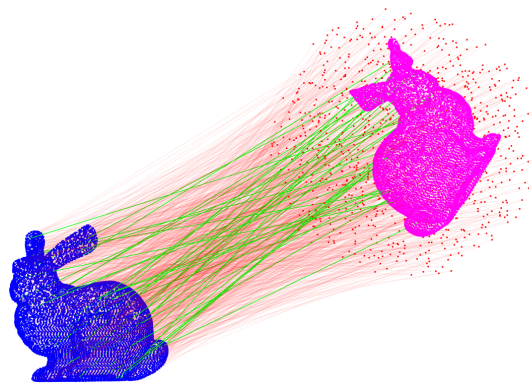


Fig. 1. The Bunny dataset [1] used in our evaluation. The inlier correspondences are shown as the thick green lines and the outliers as the thin red lines. Here, the outlier ratio is 96%. Image credit: [2].

pairwise scale consistency and prioritize samples with a smaller total ranking number.

- 2) We propose an efficient outlier rejection scheme that enables us to prescreen bad samples without having to compute the associated hypotheses, *i.e.*, rigid body transformation for known-scale problems and similarity transformation for unknown-scale problems. The key idea is to evaluate the *triplet scale consistency* of a given sample using precomputed data.

We conduct a thorough evaluation and demonstrate that our method leads to state-of-the-art results in point cloud registration up to 99% outlier ratio. Our code is publicly available at <https://github.com/sunghoon031/PCR-99>.

The remainder of this paper is organized as follows: First, related work is discussed in Section II. We formulate the problem in Section III and provide an overview of our method in Section IV. Section V and VI describe our method for unknown-scale and known-scale problems, respectively. We present the evaluation results in Section VII and draw conclusions in Section VIII.

II. RELATED WORK

In this section, we briefly review some of the existing robust correspondence-based methods.

Consensus Maximization Methods: Two popular methods that maximize the consensus set are RANSAC and Branch-and-Bound (BnB). RANSAC [11] and its variants (*e.g.*, [12], [13]) maximize the consensus by taking minimal samples randomly and iteratively. BnB [14], [15] finds the globally optimal solution by searching directly in the parameter space.

Both RANSAC and BnB run in exponential time in the worst case [16]. Recently, however, several RANSAC-based methods have been shown to achieve impressive robustness and speed, even at 99% outlier ratio (e.g., [17], [18], [19], [20]). In [10], a technique called guaranteed outlier removal (GORE) is proposed. This method finds the globally optimal solution, but it scales poorly, as it uses BnB as a possible subroutine. In [21], a quadratic-time GORE algorithm is proposed, which is shown to be more efficient. Our method is most similar to RANSAC-based consensus maximization methods, in that we also try to find the minimal sample of inliers iteratively. The main difference is that our sampling is done deterministically.

M-estimation Methods: M-estimation minimizes robust cost functions, down-weighting the effect of outliers iteratively [22], [23]. This method is sensitive to the initial guess and can easily get stuck in local minima. To reduce this sensitivity and increase the robustness to outliers, graduated non-convexity (GNC) can be used [24], [25]. However, this type of local iterative method is not capable of handling extreme outlier ratios (e.g., > 90%).

Graph-Based Methods: Some methods use graph theory to achieve robust point cloud registration. For example, in [16], [26], [27], graph theory is used to identify inliers based on invariance constraints. Readers interested in more recent graph-based methods are referred to [28], [29], [30], [31].

Single Rotation Averaging: Single rotation averaging (e.g., [32]) has been used to maximize the consensus set [33] or to find the rotation separately [2] in point cloud registration.

III. PROBLEM DEFINITION

Let $\{\mathbf{a}_i\}_{i=1}^n$ and $\{\mathbf{b}_i\}_{i=1}^n$ be two sets of the same number of 3D points. Let $\{\mathbf{a}_i\}_{i \in \mathcal{I}}$ and $\{\mathbf{b}_i\}_{i \in \mathcal{I}}$ be two subsets related by a similarity transformation with some noise $\{\mathbf{e}_i\}_{i \in \mathcal{I}}$, i.e.,

$$\mathbf{s}\mathbf{R}\mathbf{a}_i + \mathbf{t} + \mathbf{e}_i = \mathbf{b}_i \quad \text{for } i \in \mathcal{I}, \quad (1)$$

where \mathcal{I} is the set of inlier point correspondences. Their complements, $\{\mathbf{a}_i\}_{i \notin \mathcal{I}}$ and $\{\mathbf{b}_i\}_{i \notin \mathcal{I}}$, are not related to each other and they are considered to be the outliers. Given that \mathcal{I} is unknown, estimating $(s, \mathbf{R}, \mathbf{t})$ from $\{\mathbf{a}_i\}_{i=1}^n$ and $\{\mathbf{b}_i\}_{i=1}^n$ is called the *unknown-scale* point cloud registration problem. If s is known a priori, it is called the *known-scale* problem. In this work, we consider both problems.

IV. OVERVIEW OF PCR-99

For both known-scale and unknown-scale cases, our method consists of the following steps:

- 1) Score each point correspondence based on how likely it is to be an inlier.
- 2) Choose a sample of 3 points, prioritizing those with higher scores. Do not choose a sample that has ever been chosen before.
- 3) Check if the sample passes a basic prescreening test. If it passes, continue to the next step. Otherwise, go back to the previous step.
- 4) Compute the rotation, translation (and scale) between the two sets of 3 points using Horn's method [34].

- 5) Find all other points that fit well in the transformation model obtained from the previous step.
- 6) Repeat Step 2–5 until a sufficient number of inlier correspondences are found.
- 7) Recompute the rotation, translation (and scale) using all the inlier correspondences. For this step, we again use Horn's method [34].

The novel contribution of this work is an efficient and effective method for Step 1–3. In the next two sections, we will elaborate on these steps for each unknown-scale and known-scale case separately. Algorithm 1 delineates our method for unknown-scale problems.

V. UNKNOWN-SCALE REGISTRATION

A. Score Function (Step 1 in Section IV)

Consider two arbitrary point correspondences $(\mathbf{a}_i, \mathbf{b}_i)$ and $(\mathbf{a}_j, \mathbf{b}_j)$. If both of them are inliers, then

$$\frac{\|\mathbf{b}_i - \mathbf{b}_j\|}{\|\mathbf{a}_i - \mathbf{a}_j\|} \approx s, \quad (2)$$

where s is the unknown scale. Taking the natural logarithm on both sides, we get

$$\ln \frac{\|\mathbf{b}_i - \mathbf{b}_j\|}{\|\mathbf{a}_i - \mathbf{a}_j\|} - \ln s \approx 0. \quad (3)$$

Now, we define the *log ratio* between i and j as follows:

$$L(i, j) = \ln \frac{\|\mathbf{b}_i - \mathbf{b}_j\|}{\|\mathbf{a}_i - \mathbf{a}_j\|}. \quad (4)$$

Using this definition, we can rewrite (3) into

$$L(i, j) - \ln s \approx 0. \quad (5)$$

Point i is likely to be an inlier if the value of $|L(i, j) - \ln s|$ is small with many other points j , implying a high degree of *pairwise scale consistency*. Following this line of reasoning, one may design a score function like this:

$$S(i) = - \sum_{j=1}^n \min(|L(i, j) - \ln s|, \epsilon), \quad (6)$$

where ϵ is some threshold. We truncate $|L(i, j) - \ln s|$ to limit the influence of outliers. The negative sign is added because we want the score to be high when this truncated cost is low. The problem with the score function (6) is that the scale s is unknown. We solve this problem by modifying (6) as follows:

$$S(i) = - \min_{\ln s} \sum_{j=1}^n \min(|L(i, j) - \ln s|, \epsilon). \quad (7)$$

This means that we implicitly find s such that the score function is maximized. This usually works well because the score is highest when point i is an inlier, and at the same time, s is accurate. If either one of the conditions is not met, then the score will generally be low. In our experiment, we find $S(i)$ by trying out a range of values for $\ln s \in \mathcal{A}$ where

$$\mathcal{A} = \{p_i, p_i + \Delta_i, p_i + 2\Delta_i, p_i + 3\Delta_i, \dots, q_i\}, \quad (8)$$

Algorithm 1: PCR-99 for unknown-scale problems

Input: Corresponding 3D point sets $\{\mathbf{a}_i\}_{i=1}^n$ and $\{\mathbf{b}_i\}_{i=1}^n$, Inlier threshold δ_{in} .
Output: Similarity transformation $(s, \mathbf{R}, \mathbf{t})$.

```
/* Compute the log ratio matrix (Sec. V-A): */
1  $L \leftarrow \mathbf{0}_{n \times n}$ ;
2 for every possible pair  $(i, j)$  do
3    $L(i, j) \leftarrow \ln(\|\mathbf{b}_i - \mathbf{b}_j\| / \|\mathbf{a}_i - \mathbf{a}_j\|)$ ;
/* Score the correspondences (Sec. V-A): */
4  $S \leftarrow \mathbf{0}_{1 \times n}$ ;
5 for  $i = 1, 2, 3, \dots, n$  do
6   Obtain  $\mathcal{A}$  using (8)–(10);
7    $S(i) \leftarrow -\min_{\ln s \in \mathcal{A}} \sum_{j=1}^n \min(|L(i, j) - \ln s|, 0.1)$ ;
/* Generate and evaluate 3-point samples one
   by one (Sec. V-B and V-C): */
8 By sorting  $S$  in a descending order, obtain the
   ranking numbers  $r_i$  for  $i = 1, 2, \dots, n$ ;
9  $\mathcal{I}_{\text{largest}} \leftarrow \{\}$ ;  $n_{\text{hypothesis}} \leftarrow 0$ ;
10 for  $r_{\text{sum}} = 6, 7, \dots, 3n - 3$  do
11    $(r_i)_{\text{L}} \leftarrow \max(1, r_{\text{sum}} - 2n + 1)$ ;
12    $(r_i)_{\text{U}} \leftarrow \text{floor}((r_{\text{sum}} - 3)/3)$ ;
13   for  $r_i = (r_i)_{\text{L}}, \dots, (r_i)_{\text{U}}$  do
14      $(r_j)_{\text{L}} = \max(r_i + 1, r_{\text{sum}} - r_i - n)$ ;
15      $(r_j)_{\text{U}} = \text{floor}((r_{\text{sum}} - r_i - 1)/2)$ ;
16     for  $r_j = (r_j)_{\text{L}}, \dots, (r_j)_{\text{U}}$  do
17        $r_k \leftarrow r_{\text{sum}} - r_i - r_j$ ;
18       Find  $(i, j, k)$  that corresponds to
          $(r_i, r_j, r_k)$ ;
19       if  $(i, j, k)$  does not pass all of (24)–(26)
         then
20         Continue;
21       Compute  $(s, \mathbf{R}, \mathbf{t})$  from  $(i, j, k)$  using
         [34];
22        $\mathcal{I} \leftarrow$  All points that fit well in  $(s, \mathbf{R}, \mathbf{t})$ 
         under the given inlier threshold  $\delta_{\text{in}}$ ;
23       if  $n(\mathcal{I}) > n(\mathcal{I}_{\text{largest}})$  then
24          $\mathcal{I}_{\text{largest}} \leftarrow \mathcal{I}$ ;
25        $n_{\text{hypothesis}} \leftarrow n_{\text{hypothesis}} + 1$ ;
26       if  $n_{\text{hypothesis}}$  is a multiple of 1000 then
27         if  $n(\mathcal{I}_{\text{largest}}) \geq \max(9, 0.009n)$  then
28           Compute  $(s, \mathbf{R}, \mathbf{t})$  from  $\mathcal{I}_{\text{largest}}$ 
           using [34];
29           return  $(s, \mathbf{R}, \mathbf{t})$ 
```

$$p_i = \min_j L(i, j), \quad q_i = \max_j L(i, j), \quad (9)$$

$$\Delta_i = \frac{q_i - p_i}{\max\left(1, \text{Nearest integer of}\left(\frac{q_i - p_i}{0.1}\right)\right)}. \quad (10)$$

We score each point correspondence using (7). To speed up the process, we precompute $L(i, j)$ for every possible pair (i, j) and store the data in a 2D matrix. With a slight abuse of notation, we use L to denote this matrix and $L(i, j)$ to denote the entry of index (i, j) . Since $L(i, j) = L(j, i)$ according to (4), precomputing the matrix L allows us to

avoid redundant operations. Also, this data can be reused for the prescreening test, which will be discussed in Section V-C. In that section, we will also explain why we chose to take the logarithm in (3).

In Alg. 1, the log ratio matrix L is computed in line 1–3 and the correspondences are scored in line 4–7.

B. Sample Ordering (Step 2 in Section IV)

Once every point correspondence is scored, we sort them in a descending order and assign ranking numbers (r_i) to them: The one with the highest score is given a ranking number 1, and the one with the lowest score n . Then, we evaluate the sample with the smallest sum of ranking numbers first, and the one with the largest sum last. Note that the smallest sum is $1 + 2 + 3 = 6$ and the largest sum is $(n - 2) + (n - 1) + n = 3n - 3$. In the following, we outline the procedure (which corresponds to Step 2 in Section IV):

- 2.1) If Step 2 has been reached for the very first time, set $r_{\text{sum}} = 6$.
 - 2.2) Choose a sample of 3 points (i, j, k) such that $r_i + r_j + r_k = r_{\text{sum}}$. Do not choose a sample that has ever been chosen before. If no sample can be chosen and $r_{\text{sum}} < 3n - 3$, add 1 to r_{sum} and try again. We provide the implementation details in the appendix.
 - 2.3) Pass the sample on to Step 3 in Section IV.
- This procedure corresponds to line 10–18 of Alg. 1.

C. Prescreening Test (Step 3 in Section IV)

Consider a sample of three point correspondences $(\mathbf{a}_i, \mathbf{b}_i)$, $(\mathbf{a}_j, \mathbf{b}_j)$ and $(\mathbf{a}_k, \mathbf{b}_k)$. The distances between the points within each set are given by:

$$a_{ij} = \|\mathbf{a}_i - \mathbf{a}_j\|, \quad b_{ij} = \|\mathbf{b}_i - \mathbf{b}_j\|, \quad (11)$$

$$a_{jk} = \|\mathbf{a}_j - \mathbf{a}_k\|, \quad b_{jk} = \|\mathbf{b}_j - \mathbf{b}_k\|, \quad (12)$$

$$a_{ki} = \|\mathbf{a}_k - \mathbf{a}_i\|, \quad b_{ki} = \|\mathbf{b}_k - \mathbf{b}_i\|. \quad (13)$$

If all of the three correspondences are inliers, then the triangle formed by $(\mathbf{a}_i, \mathbf{a}_j, \mathbf{a}_k)$ would be almost similar to that formed by $(\mathbf{b}_i, \mathbf{b}_j, \mathbf{b}_k)$. This means that

$$\frac{a_{ij}}{b_{ij}} \approx \frac{a_{jk}}{b_{jk}} \approx \frac{a_{ki}}{b_{ki}}, \quad (14)$$

and equivalently,

$$\frac{a_{ij}}{a_{jk}} \approx \frac{b_{ij}}{b_{jk}}, \quad \frac{a_{jk}}{a_{ki}} \approx \frac{b_{jk}}{b_{ki}}, \quad \frac{a_{ij}}{a_{ki}} \approx \frac{b_{ij}}{b_{ki}}, \quad (15)$$

One could turn (14) and (15) into the following necessary conditions for inliers:

$$\left| \frac{a_{ij}}{b_{ij}} - \frac{a_{jk}}{b_{jk}} \right| < \delta, \quad \left| \frac{a_{jk}}{b_{jk}} - \frac{a_{ki}}{b_{ki}} \right| < \delta, \quad \left| \frac{a_{ij}}{b_{ij}} - \frac{a_{ki}}{b_{ki}} \right| < \delta, \quad (16)$$

$$\left| \frac{b_{ij}}{a_{ij}} - \frac{b_{jk}}{a_{jk}} \right| < \delta, \quad \left| \frac{b_{jk}}{a_{jk}} - \frac{b_{ki}}{a_{ki}} \right| < \delta, \quad \left| \frac{b_{ij}}{a_{ij}} - \frac{b_{ki}}{a_{ki}} \right| < \delta, \quad (17)$$

$$\left| \frac{a_{ij}}{a_{jk}} - \frac{b_{ij}}{b_{jk}} \right| < \delta, \quad \left| \frac{a_{jk}}{a_{ki}} - \frac{b_{jk}}{b_{ki}} \right| < \delta, \quad \left| \frac{a_{ij}}{a_{ki}} - \frac{b_{ij}}{b_{ki}} \right| < \delta, \quad (18)$$

$$\left| \frac{a_{jk}}{a_{ij}} - \frac{b_{jk}}{b_{ij}} \right| < \delta, \quad \left| \frac{a_{ki}}{a_{jk}} - \frac{b_{ki}}{b_{jk}} \right| < \delta, \quad \left| \frac{a_{ki}}{a_{ij}} - \frac{b_{ki}}{b_{ij}} \right| < \delta, \quad (19)$$

where δ is some threshold. Given samples of triplets (i, j, k) , checking (16)–(19) can be useful for selecting potential inliers. However, this can become computationally demanding as the number of samples increases (*e.g.*, due to high outlier ratios). To mitigate this issue, we take an alternative approach: We combine (14) and (15) and rewrite them as follows:

$$\frac{b_{ij}a_{jk}}{a_{ij}b_{jk}} \approx 1, \quad \frac{b_{jk}a_{ki}}{a_{jk}b_{ki}} \approx 1, \quad \frac{b_{ij}a_{ki}}{a_{ij}b_{ki}} \approx 1. \quad (20)$$

Taking the logarithm on both sides, we get

$$\ln(b_{ij}/a_{ij}) - \ln(b_{jk}/a_{jk}) \approx 0, \quad (21)$$

$$\ln(b_{jk}/a_{jk}) - \ln(b_{ki}/a_{ki}) \approx 0, \quad (22)$$

$$\ln(b_{ij}/a_{ij}) - \ln(b_{ki}/a_{ki}) \approx 0. \quad (23)$$

We turn (21)–(23) into the following necessary conditions for inliers:

$$|L(i, j) - L(j, k)| < \epsilon, \quad (24)$$

$$|L(i, k) - L(k, i)| < \epsilon, \quad (25)$$

$$|L(i, j) - L(k, i)| < \epsilon, \quad (26)$$

where ϵ is the same threshold¹ used for (6) and (7) and $L(\cdot, \cdot)$ is the log ratio defined in (4). Essentially, these conditions check the *triplet scale consistency* of a sample (i, j, k) . Since we have already computed and stored the log ratios in matrix L (as discussed in Section V-A), checking (24)–(26) is much faster than checking (16)–(19)². This is why we use the log ratio for the prescreening test, as well as the score function (7). The prescreening test is done in line 19–20 of Alg. 1.

VI. KNOWN-SCALE REGISTRATION

When the relative scale s between the two 3D point sets is known, we simply modify our method as follows:

- 1) We use (6) instead of (7) for the score function, replacing line 6–7 of Alg. 1.
- 2) We replace the prescreening conditions (24)–(26) in line 19 of Alg. 1 with

$$|L(i, j) - \ln s| < \epsilon, \quad (27)$$

$$|L(j, k) - \ln s| < \epsilon, \quad (28)$$

$$|L(k, i) - \ln s| < \epsilon. \quad (29)$$

- 3) In line 21 and 28 of Alg. 1, we do not compute s .

VII. RESULTS

We compare our method, PCR-99, against six open-source state-of-the-art methods: RANSIC [17], ICOS [18], DANIEL [19], TriVoC [35], VODRAC [20] and VOCRA [33]. We chose these methods for benchmarking, as they are claimed to be fast and robust up to 99% outliers. RANSAC [11], FGR [25], GORE [10], GNC-TLS [24] and TEASER [16] are not included in the evaluation, as they are shown to

¹In our experiments, we set $\epsilon = 0.1$.

²The proposed conditions (24)–(26) are not necessarily equivalent to (16)–(19). In practice, one may use either set of conditions by specifying appropriate thresholds δ and ϵ . We simply chose to use (24)–(26) for efficiency reasons.

		R error > 5°	R error > 10°
Unknown scale	RANSIC [17]	79 out of 5500	79 out of 5500
	ICOS [18]	12 out of 5500	11 out of 5500
	PCR-99 (no S/O)	1 out of 5500	0 out of 5500
	PCR-99	0 out of 5500	0 out of 5500
Known scale	RANSIC [17]	81 out of 5500	78 out of 5500
	ICOS [18]	24 out of 5500	22 out of 5500
	DANIEL [19]	5 out of 5500	3 out of 5500
	TriVoC [35]	2 out of 5500	0 out of 5500
	VODRAC [20]	9 out of 5500	2 out of 5500
	VOCRA [33]	16 out of 5500	16 out of 5500
	PCR-99 (no S/O)	4 out of 5500	0 out of 5500
	PCR-99	4 out of 5500	0 out of 5500

TABLE I

THE NUMBER OF TIMES LARGE ERRORS ARE PRODUCED. PCR-99 ALWAYS ACHIEVES THE BEST OR THE SECOND BEST RESULTS.

		Speedup
Unknown scale	RANSIC [17]	16
	ICOS [18]	7.0
	PCR-99 (no S/O)	1.6
Known scale	RANSIC [17]	162
	ICOS [18]	33
	DANIEL [19]	8.0
	TriVoC [35]	1.4
	VODRAC [20]	3.0
	VOCRA [33]	1.2
PCR-99 (no S/O)	9.3	

TABLE II

MEDIAN SPEEDUP OF PCR-99 COMPARED TO THE OTHER METHODS AT 99% OUTLIER RATIO.

be outperformed by the aforementioned methods (when parallelization is disabled for the fair runtime evaluation) [17], [18], [19], [35], [20], [33]. We also compare our method with an alternative version that adopts random sampling (as in RANSAC [11]) instead of the method described in Section V-B. At 99% outlier ratio, RANSIC and ICOS sometimes take hours to find a good solution. To prevent excessive computation times, we limit the iterations to 100 seconds for all methods. For known-scale problems, we evaluate all of the aforementioned methods. For unknown-scale problems, we only evaluate PCR-99 (with or without sample ordering), RANSIC and ICOS, as the other four methods are not applicable. All experiments are conducted in MATLAB on a laptop with i7-7700HQ (2.8 GHz) and 16 GB RAM.

A. Unknown-Scale Registration

We use the Bunny dataset from the Stanford 3D scanning repository [1]. The dataset is processed as follows: First, the ground-truth point cloud is obtained by downsampling the

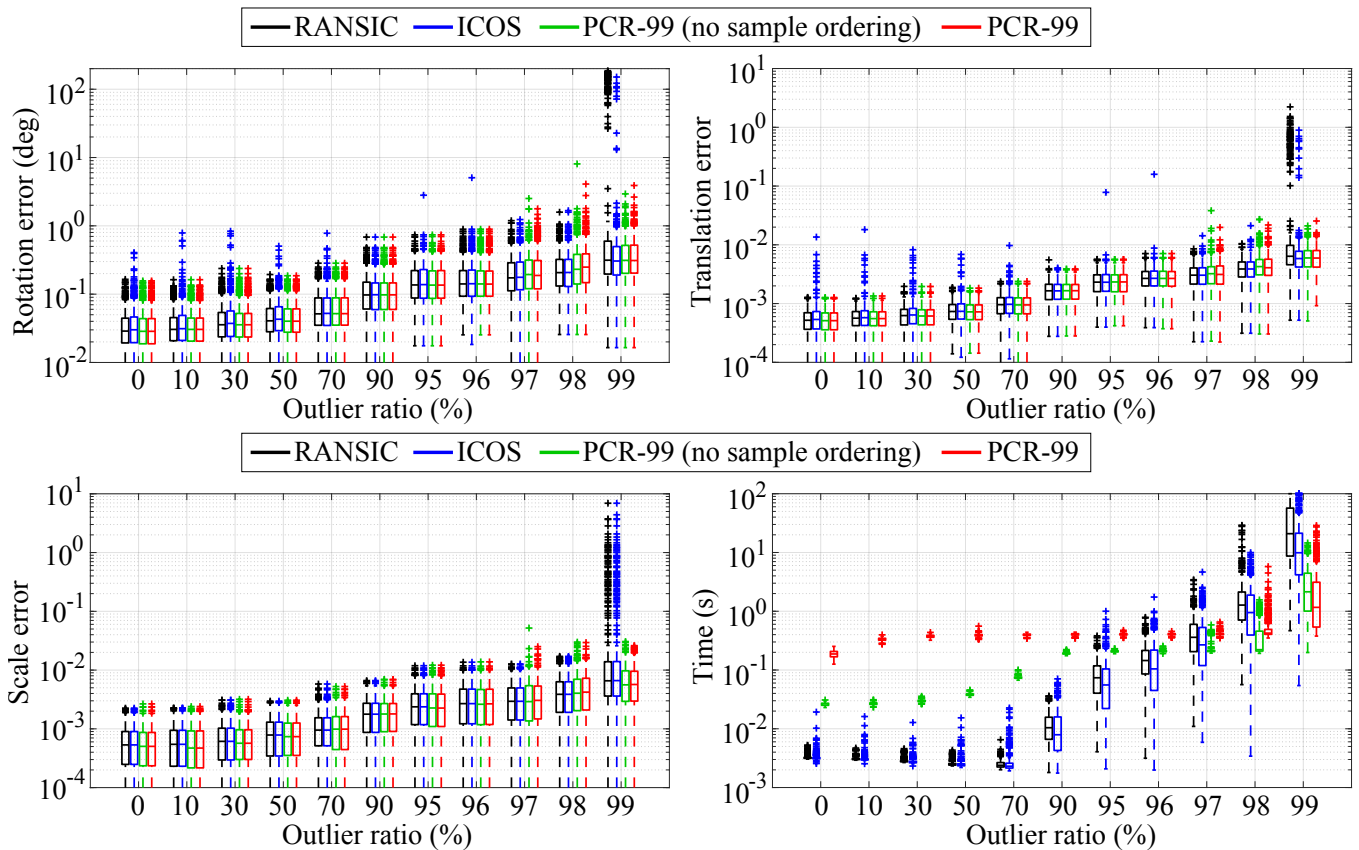


Fig. 2. Evaluation results for **unknown-scale** problems (500 Monte Carlo runs): RANSIC and ICOS are not robust at 99% outlier ratio when the computation time is limited to 100 seconds. In contrast, PCR-99 (with or without sample ordering) is robust up to 99% outlier ratio. The sample ordering has a very small impact on the accuracy and robustness of PCR-99. Comparing the median times of the two versions of PCR-99, the random sampling approach is faster up to 98% outlier ratio, but slower at 99% outlier ratio.

data to 1000 points and scaling it to fit inside a unit cube. To obtain the query point cloud, we first transform the ground truth using a random similarity transformation with a scale s where $1 < s < 5$. We then add Gaussian noise of $\sigma = 0.01$ and replace 0–99% of the points with random points inside a 3D sphere of diameter $\sqrt{3}s$ (see Fig. 1).

Fig. 2 presents the results. At 99% outlier ratio, PCR-99 (with or without sample ordering) is the only method that achieves robust registration in 100 seconds at all times (see also Tab. I). We provide the relative speed of PCR-99 with respect to the other methods in Tab. II.

B. Known-Scale Registration

We follow the same procedure as in the previous section to simulate the data for known-scale problems. The only difference here is that we set $s = 1$ at all times.

Fig. 3 presents the results. At 99% outlier ratio, TriVoC, VODRAC and PCR-99 (with or without sample ordering) are the three most robust methods (see also Tab. I). In Tab. II, we also show that PCR-99 is the fastest method at this extreme outlier ratio.

VIII. CONCLUSIONS

In this work, we proposed PCR-99, a novel method for robust point cloud registration that is capable of handling

extremely large outlier ratios in an efficient manner. We first score each point correspondence based on how likely it is to be an inlier. Specifically, we adopt a novel score function that evaluates the pairwise scale consistency. After ranking the correspondences, we evaluate a sequence of 3-point samples, starting from the one with the smallest total ranking number and gradually moving towards a larger and larger number. This approach allows us to prioritize samples that are more likely to consist of inliers only. Finally, we perform a prescreening test to check the triplet scale consistency and reject bad samples as early as possible. Once we find a good sample that leads to a sufficient number of inliers, we recompute the transformation using the inlier set.

For unknown-scale problems, we demonstrated that PCR-99 is as robust as the state of the art up to 98% outlier ratio and significantly more robust and faster at 99% outlier ratio. For known-scale problems, it is as robust as the state of the art, but faster at 99% outlier ratio.

APPENDIX

Here, we elaborate on the implementation details of Step 2.2 in Section V-B. We want to find three ranking numbers r_i , r_j and r_k (where $r_i < r_j < r_k$) such that they add up to

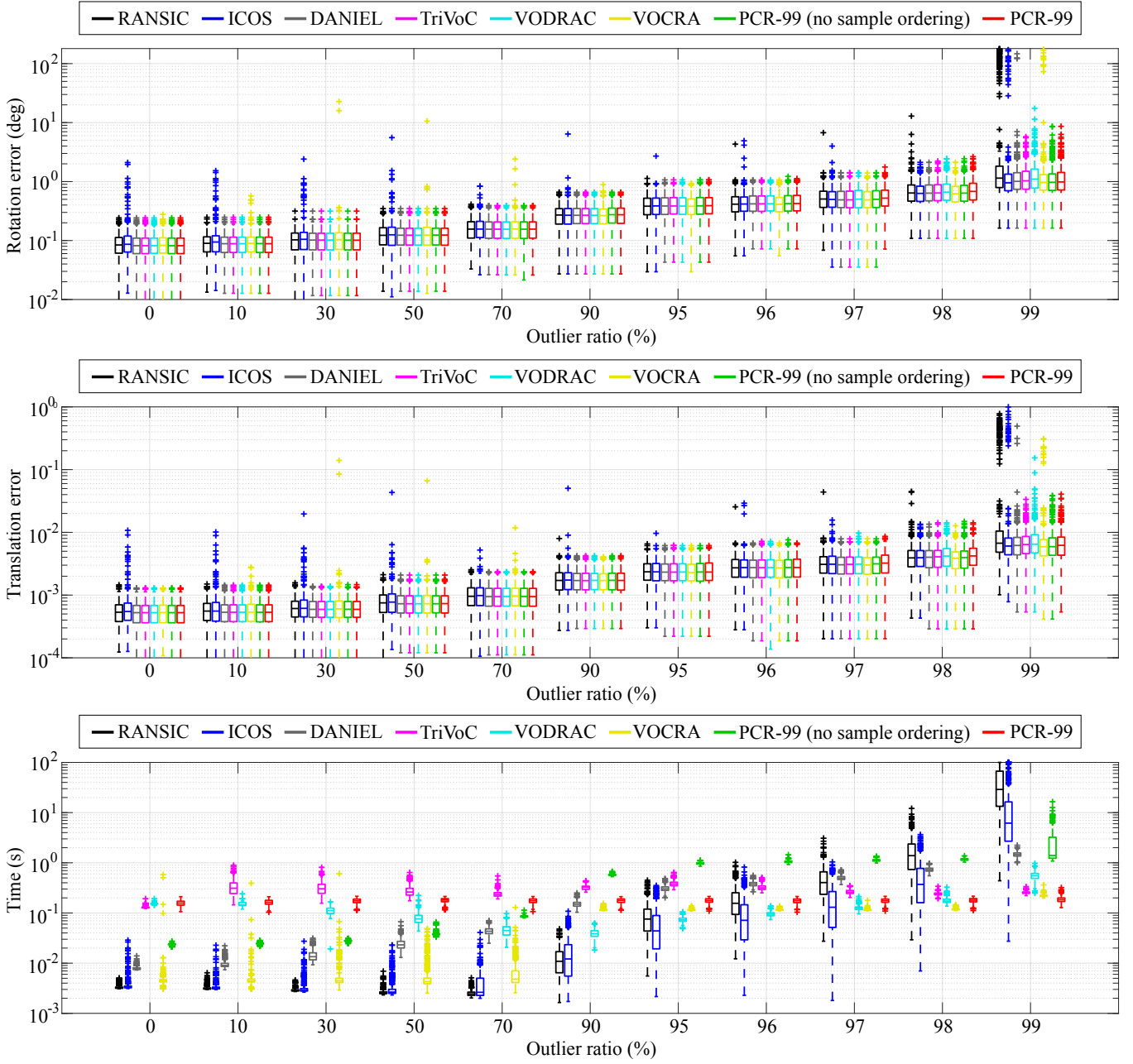


Fig. 3. Evaluation results for **known-scale** problems (500 Monte Carlo runs): TriVoC, VODRAC, and PCR-99 (with or without sample ordering) are more robust than the other methods, producing fewer large rotation errors (e.g., larger than 10°). They exhibit similar levels of robustness across all outlier ratios. For PCR-99, the sample ordering boosts the speed significantly at high outlier ratios, without causing a noticeable change in the accuracy or robustness. Among all methods, PCR-99 is the fastest one at 99% outlier ratio.

a given value, r_{sum} . They have the following constraints:

$$r_i + r_j + r_k = r_{\text{sum}}, \quad (30)$$

$$1 \leq r_i, \quad (31)$$

$$r_i + 1 \leq r_j, \quad (32)$$

$$r_j + 1 \leq r_k, \quad (33)$$

$$r_i + 2 \leq r_k, \quad (34)$$

$$r_k \leq n, \quad (35)$$

$$r_j \leq n - 1, \quad (36)$$

$$r_i \leq n - 2. \quad (37)$$

In the remainder of this section, we will manipulate (30)–(37) to obtain lower and upper bounds of r_i , r_j and r_k we can use in practice.

Adding r_i to both sides of (32) and adding (34), we get

$$3r_i + 3 \leq r_i + r_j + r_k \stackrel{(30)}{=} r_{\text{sum}}. \quad (38)$$

$$\Rightarrow r_i \leq (r_{\text{sum}} - 3)/3. \quad (39)$$

Adding r_j to both sides of (33), we get

$$2r_j + 1 \leq r_j + r_k \stackrel{(30)}{=} r_{\text{sum}} - r_i. \quad (40)$$

$$\Rightarrow r_j \leq (r_{\text{sum}} - r_i - 1)/2. \quad (41)$$

Adding (35) and (36) together, we get

$$r_j + r_k \leq 2n - 1 \stackrel{(30)}{\Rightarrow} r_{\text{sum}} - r_i \leq 2n - 1. \quad (42)$$

$$\Rightarrow r_{\text{sum}} - 2n + 1 \leq r_i. \quad (43)$$

$$\Rightarrow (r_{\text{sum}} - r_i - 1)/2 \leq n - 1. \quad (44)$$

Rewriting (35) using (30), we get

$$r_{\text{sum}} - r_i - r_j \leq n \Rightarrow r_{\text{sum}} - r_i - n \leq r_j. \quad (45)$$

Adding (35)–(37) altogether, we get

$$r_{\text{sum}} \leq 3n - 3 \Rightarrow (r_{\text{sum}} - 3)/3 \leq n - 2. \quad (46)$$

Now we are ready to derive the lower and upper bounds for r_i and r_j which can be used in practice: Combining (31), (37), (39) and (43), we get

$$\max(1, r_{\text{sum}} - 2n + 1) \leq r_i \leq \min(n - 2, (r_{\text{sum}} - 3)/3). \quad (47)$$

Combining (46) and (47), we get

$$\max(1, r_{\text{sum}} - 2n + 1) \leq r_i \leq (r_{\text{sum}} - 3)/3. \quad (48)$$

Combining (32), (36), (41) and (45), we get

$$\max(r_i + 1, r_{\text{sum}} - r_i - n) \leq r_j \leq \min\left(n - 1, \frac{r_{\text{sum}} - r_i - 1}{2}\right) \quad (49)$$

Combining (44) and (49), we get

$$\max(r_i + 1, r_{\text{sum}} - r_i - n) \leq r_j \leq (r_{\text{sum}} - r_i - 1)/2. \quad (50)$$

The inequality (48) is useful because it gives us the lower and upper bound of r_i independently of r_j and r_k . The inequality (50) is also useful because it allows us to compute the lower and upper bound of r_j once r_i is determined. Once both r_i and r_j are determined, then r_k is automatically determined using (30). Given a fixed value for r_{sum} , we produce a sequence of triplets (r_i, r_j, r_k) as follows:

- 1) In the outer loop, let r_i iterate from the lower bound $(r_i)_L$ to the upper bound $(r_i)_U$, where

$$(r_i)_L = \max(1, r_{\text{sum}} - 2n + 1), \quad (51)$$

$$(r_i)_U = \text{floor}((r_{\text{sum}} - 3)/3). \quad (52)$$

- 2) In the inner loop, let r_j iterate from the lower bound $(r_j)_L$ to the upper bound $(r_j)_U$, where

$$(r_j)_L = \max(r_i + 1, r_{\text{sum}} - r_i - n), \quad (53)$$

$$(r_j)_U = \text{floor}((r_{\text{sum}} - r_i - 1)/2), \quad (54)$$

Once r_i and r_j are determined, we can determine r_k :

$$r_k = r_{\text{sum}} - r_i - r_j. \quad (55)$$

REFERENCES

- [1] B. Curless and M. Levoy, "A volumetric method for building complex models from range images," in *SIGGRAPH*. ACM, 1996, pp. 303–312.
- [2] S. H. Lee and J. Civera, "Robust single rotation averaging revisited," *CoRR, abs/2309.05388*, 2023.
- [3] P. Henry, M. Krainin, E. Herbst, X. Ren, and D. Fox, "RGB-D mapping: Using kinect-style depth cameras for dense 3D modeling of indoor environments," *Int. J. Robot. Res.*, vol. 31, no. 5, pp. 647–663, 2012.
- [4] S. Choi, Q.-Y. Zhou, and V. Koltun, "Robust reconstruction of indoor scenes," in *IEEE Conf. Comput. Vis. Pattern Recog.*, June 2015.
- [5] B. Drost, M. Ulrich, N. Navab, and S. Ilic, "Model globally, match locally: Efficient and robust 3d object recognition," in *IEEE Conf. Comput. Vis. Pattern Recog.*, 2010, pp. 998–1005.
- [6] P. Marion, P. R. Florence, L. Manuelli, and R. Tedrake, "Label Fusion: A pipeline for generating ground truth labels for real RGBD data of cluttered scenes," in *IEEE Intl. Conf. Robot. Automat.*, 2018, pp. 1–8.
- [7] J. Zhang and S. Singh, "LOAM: Lidar odometry and mapping in real-time," in *Proc. Robotics: Science and Systems*, 2014.
- [8] P. Besl and N. D. McKay, "A method for registration of 3-d shapes," *IEEE Trans. Pattern Anal. Mach. Intell.*, vol. 14, no. 2, pp. 239–256, 1992.
- [9] R. B. Rusu, N. Blodow, and M. Beetz, "Fast point feature histograms (FPFH) for 3D registration," in *IEEE Intl. Conf. Robot. Automat.*, 2009, pp. 3212–3217.
- [10] A. Parra Bustos and T.-J. Chin, "Guaranteed outlier removal for point cloud registration with correspondences," *IEEE Trans. Pattern Anal. Mach. Intell.*, vol. 40, no. 12, pp. 2868–2882, 2018.
- [11] M. A. Fischler and R. C. Bolles, "Random sample consensus: A paradigm for model fitting with applications to image analysis and automated cartography," *Commun. ACM*, vol. 24, no. 6, pp. 381–395, 1981.
- [12] O. Chum, J. Matas, and J. Kittler, "Locally optimized RANSAC," in *Pattern Recog.*, B. Michaelis and G. Krell, Eds., 2003, pp. 236–243.
- [13] D. Nister, "Preemptive RANSAC for live structure and motion estimation," in *IEEE Int. Conf. Comput. Vis.*, vol. 1, 2003, pp. 199–206.
- [14] R. Horst and H. Tuy, *Global optimization: Deterministic approaches*. Springer Science & Business Media, 2013.
- [15] A. Parra Bustos, T.-J. Chin, A. Eriksson, H. Li, and D. Suter, "Fast rotation search with stereographic projections for 3(d) registration," *IEEE Trans. Pattern Anal. Mach. Intell.*, vol. 38, no. 11, pp. 2227–2240, 2016.
- [16] H. Yang, J. Shi, and L. Carlone, "Teaser: Fast and certifiable point cloud registration," *IEEE Trans. Robot.*, vol. 37, no. 2, pp. 314–333, 2020.
- [17] L. Sun, "RANSIC: Fast and highly robust estimation for rotation search and point cloud registration using invariant compatibility," *IEEE Robot. Automat. Lett.*, vol. 7, no. 1, pp. 143–150, 2022.
- [18] L. Sun and Z. Deng, "A fast and robust rotation search and point cloud registration method for 2d stitching and 3d object localization," *Applied Sciences*, vol. 11, no. 20, 2021.
- [19] E. Hu and L. Sun, "DANIEL: A fast and robust consensus maximization method for point cloud registration with high outlier ratios," *Information Sciences*, vol. 614, pp. 563–579, 2022.
- [20] —, "VODRAC: Efficient and robust correspondence-based point cloud registration with extreme outlier ratios," *Journal of King Saud University - Computer and Information Sciences*, vol. 35, no. 1, pp. 38–55, 2023.
- [21] J. Li, P. Shi, Q. Hu, and Y. Zhang, "QGORE: Quadratic-time guaranteed outlier removal for point cloud registration," *IEEE Trans. Pattern Anal. Mach. Intell.*, 2023.
- [22] R. Kümmerle, G. Grisetti, H. Strasdat, K. Konolige, and W. Burgard, "g2o: A general framework for graph optimization," in *IEEE Intl. Conf. Robot. Automat.*, 2011, pp. 3607–3613.
- [23] K. MacTavish and T. D. Barfoot, "At all costs: A comparison of robust cost functions for camera correspondence outliers," in *Conf. Comput. Robot. Vis.* IEEE, 2015, pp. 62–69.
- [24] H. Yang, P. Antonante, V. Tzoumas, and L. Carlone, "Graduated non-convexity for robust spatial perception: From non-minimal solvers to global outlier rejection," *IEEE Intl. Conf. Robot. Automat.*, vol. 5, no. 2, pp. 1127–1134, 2020.
- [25] Q.-Y. Zhou, J. Park, and V. Koltun, "Fast global registration," in *Eur. Conf. Comput. Vis.*, 2016, pp. 766–782.
- [26] H. Yang and L. Carlone, "A polynomial-time solution for robust registration with extreme outlier rates," in *Proc. Robotics: Science and Systems*, 2019.

[1] B. Curless and M. Levoy, "A volumetric method for building complex models from range images," in *SIGGRAPH*. ACM, 1996, pp. 303–

- [27] J. Shi, H. Yang, and L. Carlone, "ROBIN: a graph-theoretic approach to reject outliers in robust estimation using invariants," in *IEEE Intl. Conf. on Robotics and Automation (ICRA)*, 2021, pp. 13 820–13 827.
- [28] X. Bai, Z. Luo, L. Zhou, H. Chen, L. Li, Z. Hu, H. Fu, and C.-L. Tai, "PointDSC: Robust point cloud registration using deep spatial consistency," in *IEEE Conf. Comput. Vis. Pattern Recog.*, 2021, pp. 15 854–15 864.
- [29] Z. Chen, K. Sun, F. Yang, and W. Tao, "SC2-PCR: A second order spatial compatibility for efficient and robust point cloud registration," in *IEEE Conf. Comput. Vis. Pattern Recog.*, 2022, pp. 13 211–13 221.
- [30] X. Zhang, J. Yang, S. Zhang, and Y. Zhang, "3D registration with maximal cliques," in *IEEE Conf. Comput. Vis. Pattern Recog.*, 2023, pp. 17 745–17 754.
- [31] Y. Wu, X. hu, Y. Yuan, X. Fan, M. Gong, H. Li, M. Zhang, Q. Miao, and W. Ma, "PointMC: Multi-instance point cloud registration based on maximal cliques," in *Forty-first International Conference on Machine Learning*, 2024.
- [32] S. H. Lee and J. Civera, "Robust single rotation averaging," *CoRR*, *abs/2004.00732*, 2020.
- [33] L. Sun, "Practical, fast and robust point cloud registration for scene stitching and object localization," *IEEE Access*, vol. 10, pp. 3962–3978, 2022.
- [34] B. K. P. Horn, "Closed-form solution of absolute orientation using unit quaternions," *Journal of the Optical Society of America A*, vol. 4, no. 4, pp. 629–642, 1987.
- [35] L. Sun and L. Deng, "TriVoC: Efficient voting-based consensus maximization for robust point cloud registration with extreme outlier ratios," *IEEE Robot. Automat. Lett.*, vol. 7, no. 2, pp. 4654–4661, 2022.